

# UC San Diego

## UC San Diego Previously Published Works

### Title

Nicotine inhalant via E-cigarette facilitates sensorimotor function recovery by upregulating neuronal BDNF—TrkB signalling in traumatic brain injury

### Permalink

<https://escholarship.org/uc/item/86t445jt>

### Authors

Wang, Dongsheng

Li, Xiaojing

Li, Wenxi

et al.

### Publication Date

2024-05-02

### DOI

10.1111/bph.16395

Peer reviewed

## RESEARCH ARTICLE



# Nicotine inhalant via E-cigarette facilitates sensorimotor function recovery by upregulating neuronal BDNF–TrkB signalling in traumatic brain injury

Dongsheng Wang<sup>1,2</sup> | Xiaojing Li<sup>1,2</sup> | Wenxi Li<sup>1,2</sup> | Tiffany Duong<sup>1,2</sup> |  
 Hongxia Wang<sup>1,2</sup> | Natalia Kleschevnikova<sup>1,2</sup> | Hemal H. Patel<sup>1,2</sup> | Ellen Breen<sup>3</sup> |  
 Susan Powell<sup>4,5</sup> | Shanshan Wang<sup>1,2</sup> | Brian P. Head<sup>1,2</sup>

<sup>1</sup>Department of Anesthesiology, VA San Diego Healthcare System, San Diego, California, USA

<sup>2</sup>Department of Anesthesiology, University of California San Diego, La Jolla, California, USA

<sup>3</sup>Department of Medicine, Division of Pulmonary Critical Care and Sleep Medicine, University of California San Diego, La Jolla, California, USA

<sup>4</sup>Research Service and Desert Pacific Mental Illness Research, Education & Clinical Center, Veterans Affairs San Diego Health System, San Diego, California, USA

<sup>5</sup>Department of Psychiatry, University of California San Diego, La Jolla, California, USA

## Correspondence

Shanshan Wang and Brian P. Head,  
 Department of Anesthesiology, University of California San Diego, La Jolla, CA, USA, 92093.  
 Email: [shw049@health.ucsd.edu](mailto:shw049@health.ucsd.edu) and [bhead@health.ucsd.edu](mailto:bhead@health.ucsd.edu)

## Funding information

(TRDRP 2020 T311R1834 to BPH, VA Merit BX003671 and VA RCS BX006318 to BPH, AL210059 to BPH, Craig H. Neilsen Foundation 886964 to SW and BX005229 to HHP).

## Abstract

**Background and Purpose:** Traumatic brain injury (TBI) causes lifelong physical and psychological dysfunction in affected individuals. The current study investigated the effects of chronic nicotine exposure via E-cigarettes (E-cig) (vaping) on TBI-associated behavioural and biochemical changes.

**Experimental Approach:** Adult C57/BL6J male mice were subjected to controlled cortical impact (CCI) followed by daily exposure to E-cig vapour for 6 weeks. Sensorimotor functions, locomotion, and sociability were subsequently evaluated by nesting, open field, and social approach tests, respectively. Immunoblots were conducted to examine the expression of mature brain-derived neurotrophic factor (mBDNF) and associated downstream proteins (p-Erk, p-Akt). Histological analyses were performed to evaluate neuronal survival and neuroinflammation.

**Key Results:** Post-injury chronic nicotine exposure significantly improved nesting performance in CCI mice. Histological analysis revealed increased survival of cortical neurons in the perilesion cortex with chronic nicotine exposure. Immunoblots revealed that chronic nicotine exposure significantly up-regulated mBDNF, p-Erk and p-Akt expression in the perilesion cortex of CCI mice. Immunofluorescence microscopy indicated that elevated mBDNF and p-Akt expression were mainly localized within cortical neurons. Immunolabelling of Iba1 demonstrated that chronic nicotine exposure attenuated microglia-mediated neuroinflammation.

**Conclusions and Implications:** Post-injury chronic nicotine exposure via vaping facilitates recovery of sensorimotor function by upregulating neuroprotective mBDNF/TrkB/Akt/Erk signalling. These findings suggest potential neuroprotective properties

**Abbreviations:** AD, Alzheimer's Disease; AP, anterior–posterior; CCI, controlled cortical impact; CCI-Nic, CCI surgery group exposed to nicotine vapour; CCI-Veh, CCI surgery group exposed to vehicle vapour; E-cig, E-cigarette; Em, emission; Ex, excitation; Iba-1, ionized calcium-binding adaptor molecule 1; ML, medial-lateral; MS, multiple sclerosis; NeuN, neuronal nuclear protein; OF, open field test; p-TrkB, phosphorylated tropomyosin-related kinase receptor type B; S1, the primary somatosensory cortex; SA, social approach; Sham-Nic, Sham-surgerized mice exposed to nicotine vapour; Sham-Veh, Sham-surgerized mice exposed to vehicle vapour; TBI, traumatic brain injury.

Dongsheng Wang has first authorship.

This is an open access article under the terms of the [Creative Commons Attribution-NonCommercial-NoDerivs](https://creativecommons.org/licenses/by-nc-nd/4.0/) License, which permits use and distribution in any medium, provided the original work is properly cited, the use is non-commercial and no modifications or adaptations are made.

© 2024 The Authors. *British Journal of Pharmacology* published by John Wiley & Sons Ltd on behalf of British Pharmacological Society.

of nicotine despite its highly addictive nature. Thus, understanding the multifaceted effects of chronic nicotine exposure on TBI-associated symptoms is crucial for paving the way for informed and properly managed therapeutic interventions.

#### KEYWORDS

BDNF, E-cigarette, neuroprotection, nicotine, sensorimotor function, traumatic brain injury

## 1 | INTRODUCTION

Traumatic brain injury (TBI) is one of the leading causes of disability and death in the United States. According to the Centers for Disease Control and Prevention (CDC), over 220,000 TBI-related hospitalizations were documented in 2019, with 64,362 deaths attributed to TBI in 2020 alone. The primary injury from TBI is caused by a strong and abrupt mechanical force that damages the brain parenchyma. Immediate consequences include haemorrhage, neuronal damage, and disruption of the blood–brain barrier (BBB), followed by secondary injuries arising from impaired BBB, chronic inflammation and excitotoxicity. These secondary injuries further exacerbate neuronal cell death, triggering neurodegeneration and increasing the risk of neurodegenerative disorders (Brett et al., 2022).

While it is clear that premorbid use of tobacco adversely influences neurocognitive and functional outcomes in TBI, primarily due to systemic effects that can compromise brain functions and weaken the integrity of the BBB (Durazzo et al., 2013), the effects of smoking post-TBI remain elusive. A recent study that recruited 336 Veterans with TBI reported that 28% of participants were actively smoking after TBI, with 12% of preinjury non-smokers adopting smoking post-TBI (Silva et al., 2018). Given the notably higher prevalence of smoking among Veterans and active military members, this unique demographic group may be particularly susceptible to the combined effects of TBI and nicotine dependence. Understanding the effects of post-TBI smoking is thus essential for developing targeted interventions to improve overall outcomes.

**Nicotine**, the active ingredient in E-cig, exerts its psychoactive effects by binding to **nicotinic acetylcholine receptors** (nACh receptors) in the brain. In the central nervous system (CNS), nACh receptors play crucial roles in mediating cholinergic transmission, neurotransmitter and growth factor release (Castillo-Rolon et al., 2020; Serres & Carney, 2006). nACh receptors have been implicated in various CNS disorders, including TBI, Alzheimer's Disease (AD), Parkinson's Disease (PD) and other neurodegenerative conditions. Over the past decade, selective activation of  **$\alpha 7$  nACh receptors** to restore lost cholinergic signalling has gained increasing attention as a potential therapeutic approach to treat various neurological conditions (Dineley et al., 2015; Roberts et al., 2021). Despite preclinical studies suggesting potential neuroprotective effects of nicotine in TBI (Lee et al., 2012; Rao et al., 2022; Shin et al., 2012; Verbois, Scheff, & Pauly, 2003), it is crucial to recognize that E-cig use is still clinically recognized as a major risk factor for addiction, cancer and cardiovascular disease. Furthermore, the effects of long-term nicotine use on post-TBI recovery

### What is already known?

- Premorbid tobacco/E-cig are linked to adverse effects on functional outcomes in traumatic brain injury (TBI).
- Nicotine modulates biological activities and has been shown to afford neuroprotective effects in neurodegenerative disease.

### What does this study add?

- Chronic nicotine exposure after TBI is protective in preventing neuron loss in the perilesion cortex.
- Nicotine's neuroprotective effect is mediated by the upregulation of neuronal BDNF/TrkB signalling in the cortex.

### What is the clinical significance?

- nACh receptor-selective agonists could serve as therapeutic agents for neuroprotection against TBI and neurodegenerative diseases.
- This can be achieved without inducing the addictive side effects associated with prolonged nicotine exposure.

remain unclear; thus, a more comprehensive understanding of the molecular and cellular changes in post-injury nicotine exposure is urgently needed.

The current study aims to (1) provide a comprehensive neurobehavioral analysis of the effects of chronic nicotine exposure following TBI; (2) elucidate the molecular mechanisms underlying nicotine-induced behavioural changes in TBI mice; (3) examine the effects of post-injury chronic nicotine exposure on TBI-induced pathophysiology. Considering the prevalent use of electronic cigarettes (E-cig) in our society (Jones & Salzman, 2020), this study employs an E-cig vapour exposure model to simulate human vaping sessions. This approach enhances the relevance of the findings to current patterns of nicotine abuse and provides insights into the impact of chronic nicotine exposure after TBI.

## 2 | METHODS

### 2.1 | Animals

Three-month-old adult male C57BL/6J mice were obtained from Jackson Laboratory (Bar Harbor, ME, USA) and treated in compliance with the *Guide for the Care and Use of Laboratory Animals* (National Institutes of Health, Bethesda, MD, USA). Animal use protocols (#20-021) was approved by the Veterans Administration San Diego Healthcare System Institutional Animal Care and Use Committee (IACUC). Animal studies are reported in compliance with the ARRIVE guidelines (Percie du Sert et al., 2020) and with the recommendations made by the *British Journal of Pharmacology* (Lilley et al., 2020). Mice were housed on a 12 h:12 h light-dark cycle (lights on at 6 AM) in a temperature and humidity-controlled room with a sufficient supply of water and food. Additionally, mice were housed with littermates (3–4 mice) in standard cages (28.4 × 18.4 × 12.5 cm) floored with corn cob bedding in an individually ventilated caging system.

### 2.2 | Experimental design

Mice were randomly divided into six groups: Sham-Vehicle (Veh,  $n = 16$ ), Sham-Nicotine (Nic,  $n = 11$ ), Sham-Nicotine Withdrawal (Nic Withdrawal,  $n = 15$ ), controlled cortical impact (CCI)-Vehicle ( $n = 16$ ),

CCI-Nicotine ( $n = 20$ ) and CCI-Nicotine Withdrawal ( $n = 19$ ). Mice underwent either Sham surgery or CCI surgery first, followed by baseline assessment for social preference using the three-chambered social approach (SA) test one-week after surgery. Next, mice received daily vehicle or nicotine-containing vapour exposure for 6 weeks. Considering the short half-life of nicotine, post-exposure behavioural tests, including nesting, SA test, and open field, were performed during the last week of exposure for nicotine-exposed groups. Behavioural tests for the Withdrawal groups were conducted 1 week after the completion of the 6-week exposure period (Figure 1a). The behavioural test operator and data analysts were blinded to the experimental groups until the completion of data analysis. Animals that showed signs of distress, pain, infection at the surgical site and aggressive behaviours were excluded from all above-mentioned behavioural tests. Upon completion of behavioural test batteries, mice were killed by pentobarbital (100–120 mg·kg<sup>-1</sup>) overdose via intraperitoneal injection. A minimum of six mice per group were allocated for immunoblot analysis. A minimum of five mice per group were allocated for immunofluorescence and histological analysis.

### 2.3 | Controlled cortical impacts (CCI) model

The CCI procedure was performed as described previously (Egawa et al., 2017). Mice were anaesthetised with isoflurane (1.5% with

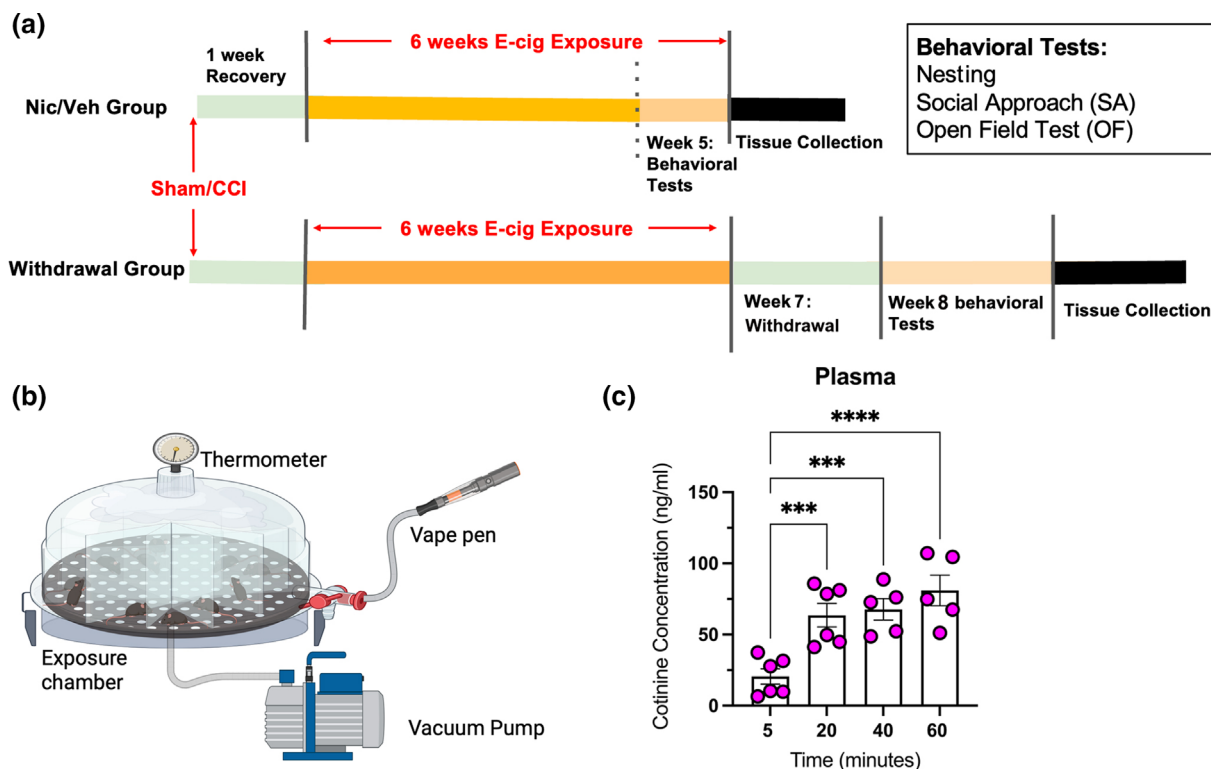


**FIGURE 1** Confirmation of nicotine delivery efficacy via a new E-cigarette vapour exposure chamber. (a) Experiment timeline. (b) Illustration of the E-cig vapour exposure chamber. (c) Cotinine concentration in blood plasma. Cotinine concentration was analysed using a one-way ANOVA followed by post hoc Fisher's LSD test. Data are presented as mean ± SEM,  $n=2-4$  per group. No statistical test was carried out where  $n < 5$ . Nic, nicotine.

oxygen at  $1 \text{ L}\cdot\text{min}^{-1}$ ) and kept on a  $37^\circ\text{C}$  heating pad during the surgery. Mice were stabilized in a stereotaxic frame, and a  $4 \text{ mm} \times 4 \text{ mm}$  cranial window (AP:  $+1$  to  $-3 \text{ mm}$ , ML:  $+0.5$  to  $+4.5 \text{ mm}$ ) was created above the right hemisphere. A 3-mm-diameter flat-tip impactor (Impact one; [myNeuroLab.com](http://myNeuroLab.com), Richmond, IL, USA) was centred on the dura and accelerated to  $3 \text{ m}\cdot\text{s}^{-1}$  to impact the brain at a depth of 1 mm below the cortical surface. Those coordinates were chosen to target the sensory and motor cortices specifically to induce major deficits in sensorimotor function. A sterilized cover glass was placed over the cranial window, and surgical clips were used to close the incision. Slow-released buprenorphine ( $1 \text{ mg}\cdot\text{kg}^{-1}$ ) was used for pain control. The animals were allowed to recover for 1 week before baseline behaviour testing and vapour exposure.

## 2.4 | Vapour exposure chamber model

A Stick V9 Max vape pen kit was used to aerosolize nicotine-containing E-liquid. The stick battery provides an output voltage of 2.1 to 4.1 V and an output power of 60 W. An E-liquid tank of 8.5-ml volume capacity is attached to the battery. The E-liquid vehicle contains 70% Vegetable Glycerin and 30% Propylene Glycol. Nicotine (#N3876,  $\geq 99\%$  [GC], Sigma-Aldrich, Burlington, USA), is added to the vehicle solution to achieve a concentration of  $24 \text{ mg}\cdot\text{ml}^{-1}$  (Alasmari et al., 2022). A paired Baby V2 S2 0.15 Ohm coil is used to create clouds of vape smoke. The mouthpiece of the vape pen is connected to the exposure chamber via polyvinyl chloride (PVC) and metal tubing for effective delivery of vape smoke. A vacuum pump set at 50 psi is used to provide ventilation and draw vapour into the chamber. Heating tapes are secured around the chamber for temperature control. A temperature probe is inserted into the chamber providing constant readouts. Each exposure session lasts 40 min, and each single puff cycle consists of 5 s of heated E-cig vapour exposure followed by 25 s of air.

## 2.5 | Determination of optimal exposure temperature and exposure duration

Previous studies have shown that chamber temperature affects the size of aerosolized particles and smoke delivery efficiency (Lechasseur et al., 2019); we thus first tested the efficiency of vapour delivery at varying chamber temperatures. Mice were exposed to vehicle vapour containing Evans Blue fluorescent dye at four different temperatures (21, 28, 32,  $36^\circ\text{C}$ ) within the animal's thermal neutral zone. Animals were killed immediately after exposure, and the lungs were imaged by an IVIS Spectrum In Vivo Imaging machine ( $E_m = 700$ ,  $E_x = 640$ ). To determine the optimal exposure duration, mice were exposed to nicotine-containing vapour for 5, 20, 40 and 60 min, respectively. Plasma samples were collected to assess cotinine concentration using the Cotinine Direct ELISA kit (Calbiotech, CO096D, San Diego, USA).

## 2.6 | Behavioural tests and analyses

### 2.6.1 | Open Field (OF)

The Open Field (OF) test was performed to assess general locomotion and anxiety-like behaviour. Mice were placed in a square arena ( $41 \times 41 \times 34 \text{ cm}$  enclosures) illuminated by a bright light. A computerized video tracking system (Noldus Ethovision XT 7.1, Leesburg, VA, USA) was used for recording during a 10-min test session. Distance moved (cm), velocity ( $\text{cm}\cdot\text{s}^{-1}$ ) and time spent in the centre of the arena (s) were recorded as previously described (Wang et al., 2021). No animals were excluded from this experiment.

### 2.6.2 | Nesting

Nest building is an innate and highly motivated behaviour performed by rodents to provide adequate thermo-regulation and to support pup survival (Gaskill et al., 2012). Since this behaviour requires intricate coordination between sensory feedback and motor outputs, which includes pulling, carrying and fluffing of the nesting material, it has been used to assess sensorimotor function in rodents (Deacon, 2006; Fleming et al., 2004; Paumier et al., 2013; Yuan et al., 2018). To measure nest building, mice were housed in single cages approximately 1 h before the start of the dark cycle. Three grams of a square-shaped nestlet (Ancare, NES3600) was placed in each cage with no other cage enrichment. Nests were scored the next day at 8 am. A nesting score is given based on the weight of the unused nestlet, and the overall shape of the nest (1:  $>90\%$  of nestlet intact; 2:  $50\%$ – $90\%$  of nestlet intact; 3:  $10\%$ – $50\%$  of nestlet intact; 4:  $<10\%$  of nestlet intact, the nest is flat; 5:  $<10\%$  of nestlet intact, the nest is identifiable with high walls). No animals were excluded from this experiment.

### 2.6.3 | Social approach (SA)

Neuropsychiatric disorders such as mood dysregulation and elevated social anxiety are commonly seen following TBI and nicotine exposure (Jobson et al., 2019). Thus, we assessed social preference before and after chronic nicotine exposure to evaluate the effects of nicotine exposure on sociability in CCI mice. The social approach (SA) test consists of a habituation stage followed by a test stage. In the habituation phase, the test mouse was given 10 min to explore the three-chambered arena with empty, inverted stainless steel wire cups (Galaxy Cup Inc. Streetsboro, OH) placed in the two outer chambers. In the test stage, a stranger mouse (pre-pubescent male) was placed under one cup located in either left or right chamber, and an object was placed under the other cup located in the opposite outer chamber (Figure 4a). The test mouse was then placed in the centre chamber and allowed to explore the entire arena for 10 min. Time spent with the stranger mouse and the non-social stimulus (object) was recorded. The sociability of the animals was evaluated by the social preference index defined by the difference between time spent

with a stranger mouse and an inanimate object divided by the total exploration time (Rein et al., 2020). Singly housed mouse and mice that demonstrates aggressive behaviour were excluded from this behavioural test.

## 2.7 | Immunoblotting (IB)

Freshly dissected cortical tissue was homogenized in cold 500-mM sodium carbonate buffer (pH 11.0; Thermo Scientific Halt Protease and phosphatase inhibitor cocktail included, #78446, USA) and sonicated three times for 10s (Wang et al., 2021). Tissue homogenates were immunoblotted using primary antibodies for **BDNF** (ProteinTech #28205-1-AP, RRID:AB\_2818984, 1:500, USA), GAPDH (Cell Signaling Technology #2118S; RRID:AB\_561053, 1:1000, USA), p-TrkB (Millipore #ABN1381, RRID:AB\_2721199, 1:500, USA); TrkB (BD Biosciences 610101; RRID:AB\_397507, 1:1000, USA), p-Akt (Cell Signaling Technology #9271L, 1:1000), Akt (Cell Signaling Technology #9272S, RRID:AB\_329827, 1:1500), p-ERK (Cell Signaling Technology #4370, RRID:AB\_2315112, 1:1500) and ERK (Cell Signaling #9102, RRID:AB\_330744, 1:1500) overnight at 4°. Subsequently, the membrane was incubated with HRP-linked anti-rabbit IgG (Cell Signaling

Technology #7074S, RRID:AB\_2099233, 1:1000) for 1 h at room temperature (RT). Lumigen ECL Ultra (Lumigen TMA-6) was used to visualize the signal, and densitometry analysis was performed using Photoshop. All bands were normalized to GAPDH, and all phosphorylated proteins were normalized to the respective total proteins.

## 2.8 | Lesion volume and neuronal survival assessment

Mice were transcardially perfused with cold PBS followed by z-fix zinc formalin fixative (Cat#182, ANATECH LTD, USA). Brains were then carefully removed for post-fixation in z-fix at 4 °C overnight, followed by dehydration in 30% sucrose on the following day. Serial 40- $\mu$ m coronal sections were collected and stained with cresyl violet stain solution (0.1%). Lesion area and neuronal count were analysed using Photoshop. Lesion size was quantified by normalizing the size of the lesion area in the ipsilateral hemisphere to the intact contralateral hemisphere to control for unwanted sources of variations from dehydration and rehydration processes during tissue processing. Lesion size measurements were calculated by using a total of five sections with 1-mm intervals starting from AP +1.4 mm to AP -2.6 mm as

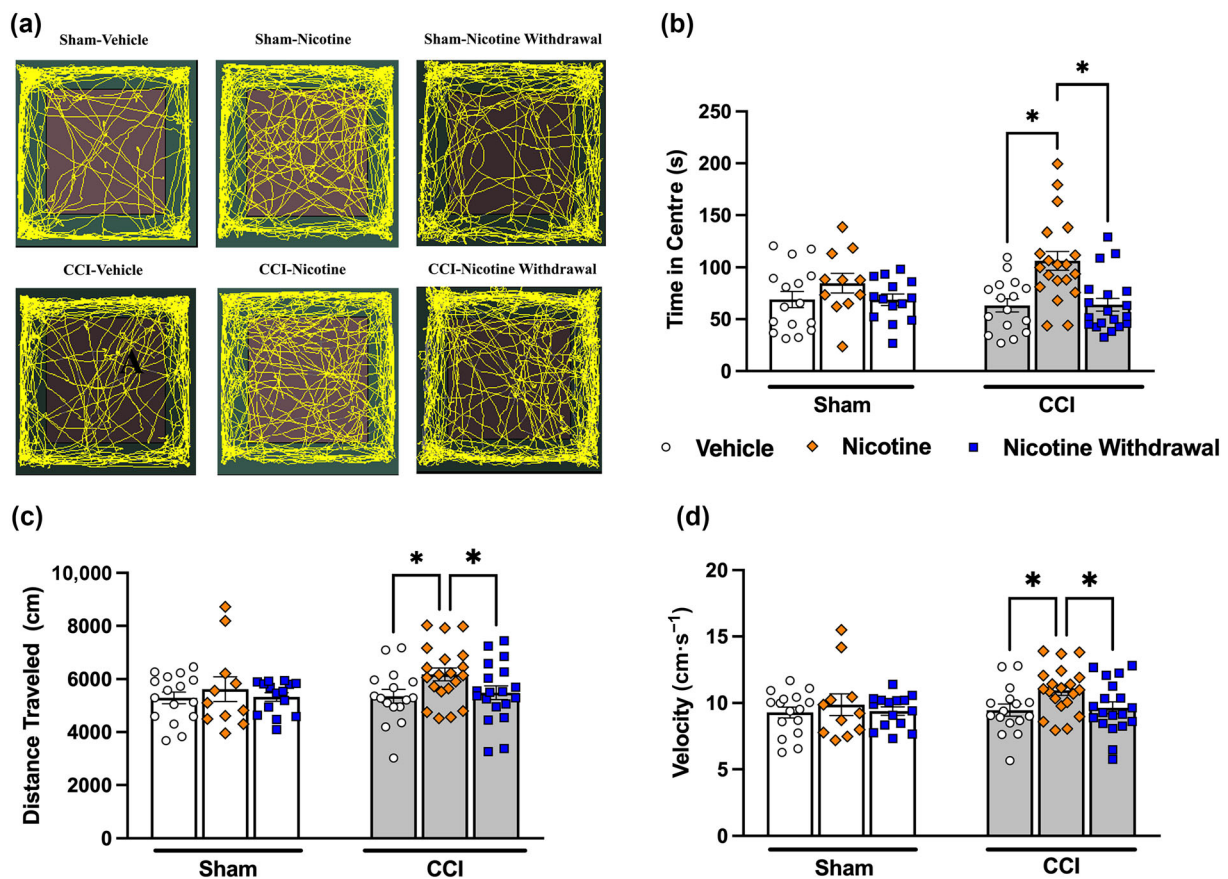


**FIGURE 2** Chronic nicotine exposure induces transient hyperactivity and anxiolytic effects in controlled cortical impact (CCI) mice. (a) Representative open field test (OF) track visualization. (b) Time in the centre of the OF arena at the end of post-exposure Week 5. (c,d) Total distance travelled and velocity of animals in the OF arena. Panels (b)–(d) are analysed using two-way ANOVA followed by post hoc Fisher's LSD comparison test. Data are presented as mean  $\pm$  SEM,  $n = 11$ –20 per group. \* $P < 0.05$ , significantly different from vehicle within Sham and CCI groups.

illustrated in Figure S5a. Lesion volume was determined by averaging lesion size from all five sections. Neuronal count analysis was performed using 40X image captured by Keyence All in One (BZ-X700, Keyence Corporation of America, IL, USA). Nissl-stained neurons were counted manually in the motor cortex at the perilesion area. Mean values were calculated from two approximately equidistant slices.

## 2.9 | Immunofluorescence microscopy (IF)

Floating sections (40  $\mu$ m thickness) were blocked in 10% goat serum in Tris-buffered saline (TBS)-Triton 0.25% solution for 1 h at RT. Subsequently, sections were incubated with primary antibodies: anti-p-Akt (Cell Signaling #9271L, 1:100), anti-Iba 1 (Wako #019-19741, RRID:AB\_839504, 1:500, Japan), and anti-neuronal nuclear protein (NeuN) (Millipore Sigma #ABN91, RRID:AB\_11205760, 1:1000) diluted in the blocking solution at 4°C for 48 h followed by incubation with species-specific fluorescent secondary antibodies in the dark for 2 h at RT. For p-akt and BDNF staining, sections were heated in 10-mM sodium citrate buffer (pH 6.0 and 0.05% Tween 20) for 20 min at 95–100°C for antigen retrieval. Next, slices were pretreated with hydrogen peroxide for 30 min prior to overnight anti-BDNF (Protein Tech #28205, 1:2000) incubation. On the following day, sections were incubated with Biotin-SP-AffiniPure Goat anti-Rabbit IgG (H+L): (Jackson ImmunoResearch Labs Cat# 111-065-003, RRID:AB\_2337959, USA) for 2 h followed

by 30 min of incubation in an Avidin-Biotin Complex solution (Vector Laboratories, PK6100). Next, sections were treated with a biotinyl tyramide solution for 20 min followed by incubation with streptavidin 647 (Invitrogen, S21374, 1:500, USA) for 2 h in the dark. The Immuno-related procedures used comply with the recommendations made by the *British Journal of Pharmacology* (Alexander et al., 2018).

## 2.10 | Microglia cell count and morphological analysis

Images of the perilesion region (500  $\mu$ m away from the lesion boundary) were captured using a 20X objective lens (PlanApo $\lambda$ , NA 0.75) with z-stack of 14  $\mu$ m thickness. Composite images were processed in Photoshop. Microglia were manually counted using the Photoshop count function and normalized to total cell counts identified by DAPI staining.

Morphological analysis of microglia process endpoints and branch length was performed using the protocol described by Young and Morrison (Young & Morrison, 2018). Three z-stacked photomicrographs of the perilesion cortex were captured for each tissue section using a 40X objective lens (Olympus P, NA 0.75). Fluorescent images were converted to 8-bit grayscale images using ImageJ. Brightness and contrast were subsequently adjusted to ensure clear and consistent visualization of microglia. The unsharp mask filter was added to increase the contrast of the image further. The de-speckle function was subsequently used to remove salt-and-pepper noise

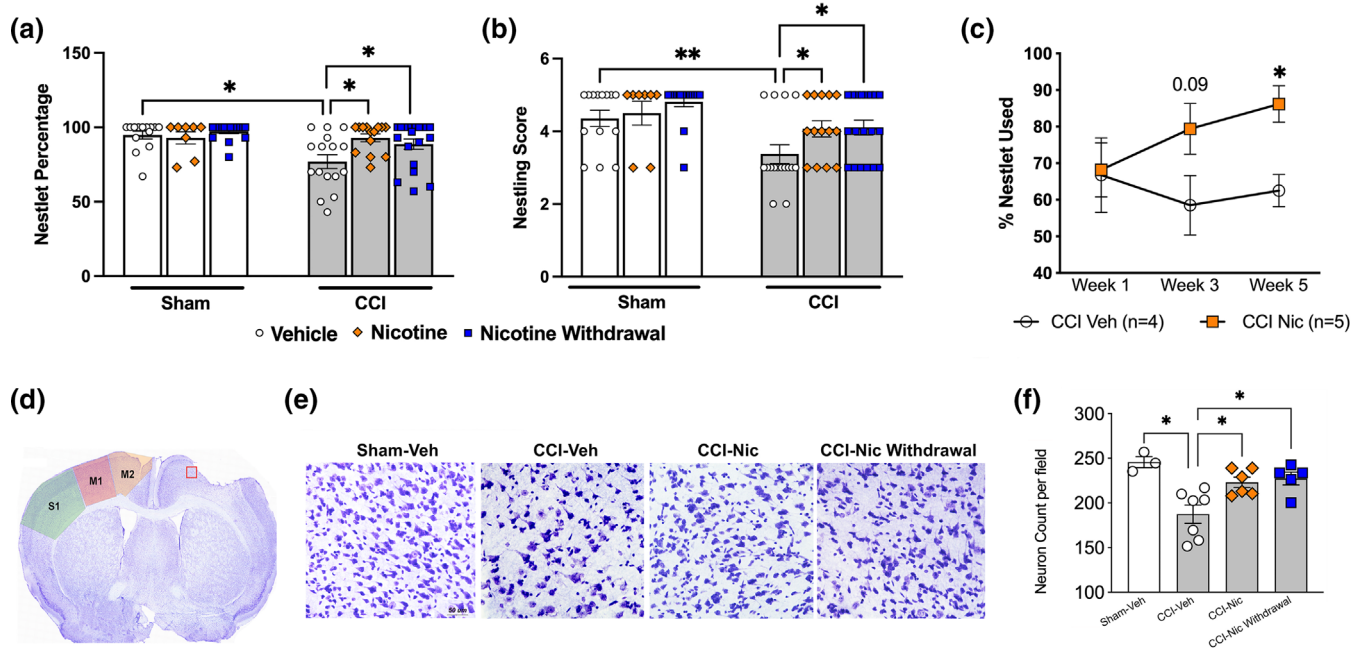


**FIGURE 3** Chronic nicotine exposure facilitates sensorimotor function recovery in controlled cortical impact (CCI) mice. (a,b) Percentage of total nestlet used and nesting score after 6 weeks exposure. (c) Biweekly nesting assessment. (d) Representative image of Nissl staining showing lesion in the motor and sensory cortex. Red box represents the selected area for neuronal count analysis. (e,f) Representative image of zoomed-in Nissl staining in the perilesion motor cortex and the quantification. Panels (a)–(c) are analysed using two-way ANOVA followed by post hoc Fisher's LSD comparison test. *F* is analysed using one-way ANOVA followed by post hoc Fisher's LSD comparison test. Data are presented as mean  $\pm$  SEM. Significance was assumed when  $*P < 0.05$ . Nic, nicotine.

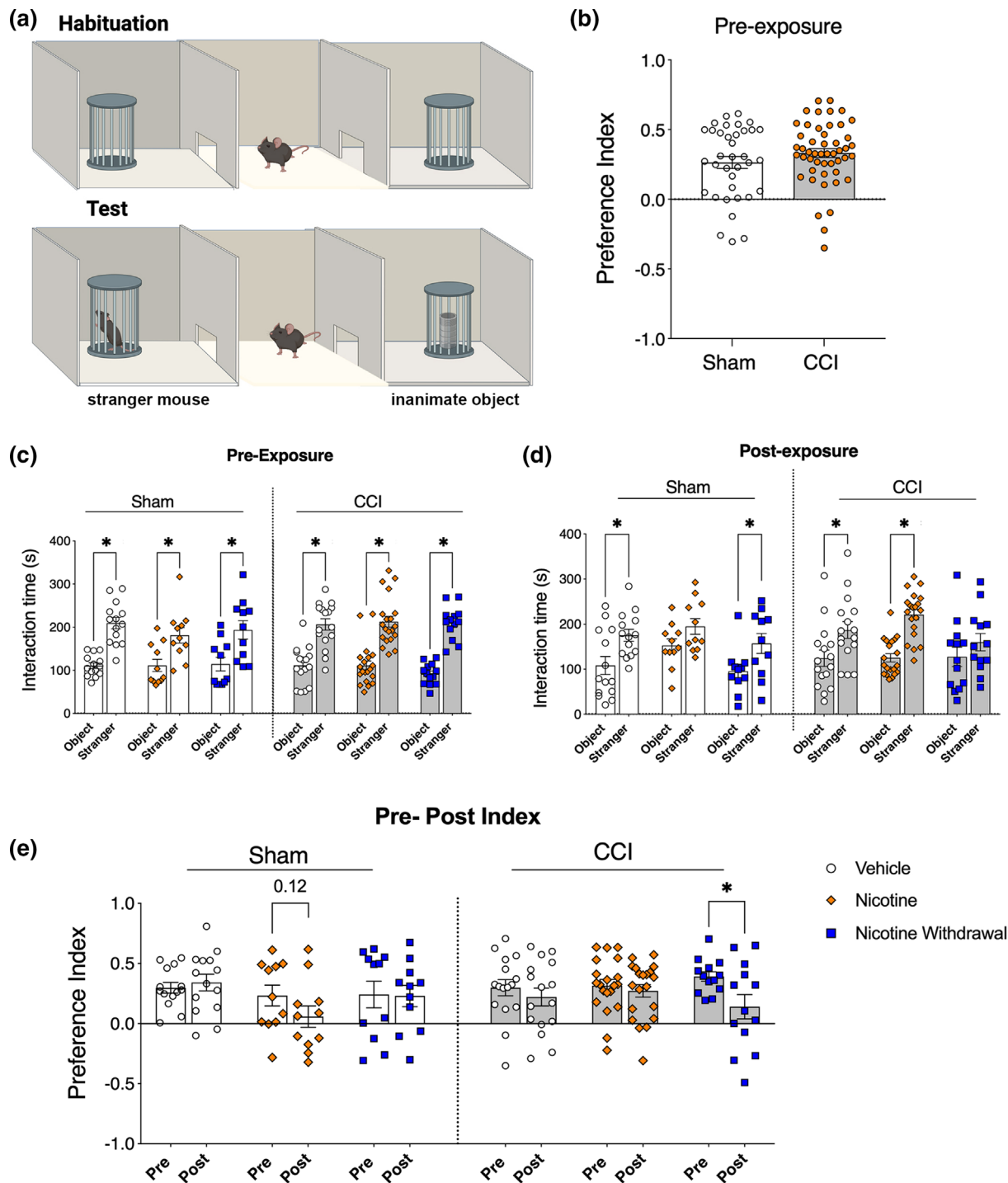


**FIGURE 4** Chronic nicotine exposure inhibits social approach behaviour. (a) Schematic diagram of the three-chambered social approach test. (b) Pre-exposure baseline social preference of Sham and controlled cortical impact (CCI) mice. (c) Interaction time with object and stranger before exposure (after Sham or CCI surgery). (d) Interaction time with object and stranger after 30-day exposure. (e) Social preference changes from pre-exposure to post-exposure time point. Panel (b) is analysed using unpaired *t* test. Panels (c)–(e) are analysed using two-way ANOVA followed by post hoc Fisher LSD's comparison test. Data are presented as mean  $\pm$  SEM. Significance was assumed when  $*P < 0.05$ .

generated by the unsharp mask filter. The image was then converted to binary using the threshold function. The de-speckle, close- and remove outlier functions were applied in sequence to remove single-pixel noise and close gaps between processes. Lastly, binary images

were skeletonized and analysed with ImageJ's Analyzeskeleton (2D/3D) function. Branch information of microglia was copied to an Excel spreadsheet for sorting and filtering. A cutoff pixel length of 0.168 was determined for undesired fragments by measuring and



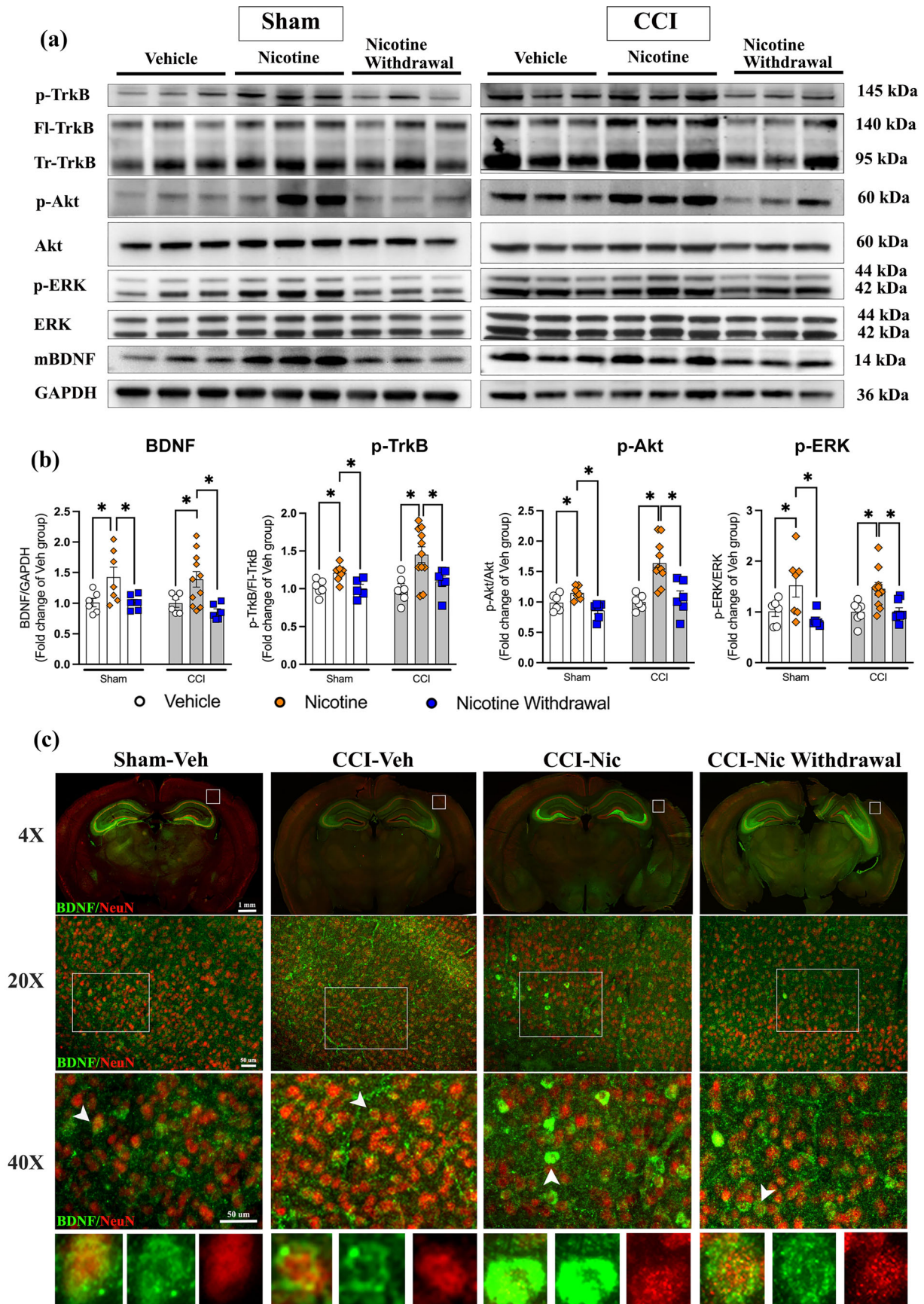


**FIGURE 5** Legend on next page.

averaging the length of six fragments using the line tool in ImageJ. The total number of microglial process endpoints was summed and normalized by the total number of microglia on the 40X micrograph. The same analysis was performed three times for each image, and the average was taken for final statistical analysis.

## 2.11 | Data analysis

Data were analysed by Student *t* tests, one-way analysis of variance (ANOVA), or two-way ANOVA followed by Fisher's LSD or Bonferroni's multiple comparisons tests as appropriate using GraphPad Prism 10 (La Jolla, California). Post-hoc tests were run only if *F* achieved  $P < 0.05$  and there was no significant variance inhomogeneity. Data were presented as mean  $\pm$  SEM, and significance was assumed when  $*P < 0.05$ . Experimental groups were blinded to the observer, and the code was broken for analysis. The statistical analysis was performed for experiments with a group size of five or more. No data points were excluded from the statistical analysis in any experiment. Data and statistical analysis complied with the recommendations of the *British Journal of Pharmacology* on experimental design and analysis in pharmacology (Curtis et al., 2022).

## 2.12 | Nomenclature of targets and ligands

Key protein targets and ligands in this article are hyperlinked to corresponding entries in <http://www.guidetopharmacology.org>, and are permanently archived in the Concise Guide to PHARMACOLOGY 2021/2022 (Alexander, Fabbro et al., 2023a,b; Alexander, Mathie et al., 2023).

# 3 | RESULT

## 3.1 | Confirmation of nicotine delivery efficacy via a new semi-automated vapour exposure chamber

The current study utilized a semiauto vapour exposure chamber to mimic human vaping (Figure 1b). As shown in Figure S1, fluorescent imaging of inflated lungs displayed no significant difference in Evans Blue Dye intensity at all four temperatures after 30 min of vapour exposure. Next, the optimal exposure duration was determined as shown in Figure 1c. Plasma cotinine level showed a significant increase after 20 min of exposure to nicotine-containing aerosol,

reaching  $63.6 \pm 8.3$  ng·ml<sup>-1</sup> at 20 min, comparable to the blood cotinine level detected in human E-cig users ( $60.6 \pm 34$  ng·ml<sup>-1</sup>) after 1 h of an active vaping session (Flouris et al., 2013). Since the plasma cotinine concentration was not statistically different among mice that were exposed to nicotine for 20, 40 and 60 min, 40-min E-cig exposure at 28°C was chosen for all following experiments to ensure efficacious and adequate delivery of nicotine.

## 3.2 | Chronic nicotine exposure induces transient hyperlocomotion and decreases thigmotactic behaviour in CCI mice

Mice generally exhibit a strong thigmotactic behaviour, a tendency to remain close to the walls of the testing arena due to a natural aversion to open space. Thus, the OF test (Figure 2a) was performed to evaluate the effects of chronic nicotine exposure on locomotor activity and anxiety-like behaviours. In the current study, while no difference was observed in all three parameters within the three Sham groups, mice from CCI-Nic group exhibited significantly increased velocity, total distance travelled and time spent in the arena centre compared to CCI-Veh and CCI-Nic Withdrawal group (Figure 2b-d), indicating that chronic nicotine exposure induced a transient increase in locomotor activity accompanied by suppressed thigmotaxis in CCI mice.

## 3.3 | Chronic nicotine exposure improves long-term sensorimotor function recovery and protects against neuronal loss in the perilesion motor cortex

We next performed the nesting test to assess sensorimotor function and the general wellness of mice after chronic nicotine exposure. Nesting performance was evaluated quantitatively and qualitatively via percent nestlet usage and nesting score, respectively. After 5 weeks of exposure, no difference in nestlet usage and nesting score was observed within Sham groups (Figure 3a,b), suggesting that chronic nicotine exposure or withdrawal did not affect the animal's tendency and ability to construct nests. Since the current CCI model causes significant tissue loss in the motor and sensory cortices, mice from the CCI-Veh group exhibited, as expected, a significant decrease in percent nestlet usage and nesting score compared to that of the Sham-Veh group. This result is consistent with a previous study using a similar chronic CCI mouse model (Ritzel et al., 2020). On the other hand, mice from CCI-Nic and CCI-Nic Withdrawal groups displayed

**FIGURE 5** Chronic nicotine exposure increases mBDNF expression and up-regulates neuronal BDNF-TrkB signalling in the ipsilateral cortex. (a) Immunoblot (IB) analyses of the expression of p-TrkB, TrkB, p-Akt, Akt, p-ERK, ERK, mBDNF and GAPDH in the ipsilateral cortex of Sham (a) and controlled cortical impact (CCI) mice. (b) Quantification of IBs in (a),  $n = 6-11$  per group. (c) Representative immunofluorescence (IF) images of BDNF (green) and neuronal marker neuronal nuclear protein (NeuN) (red). Images in the lower row show higher magnification images of the box region in the respective upper row. Bottom panel shows zoomed-in view as indicated by the arrowhead in 40X image. Data are analysed using one-way ANOVA followed by Fisher's LSD tests. Data are presented as mean  $\pm$  SEM. Significance was assumed when  $*P < 0.05$ . Veh: Vehicle; Nic: Nicotine.

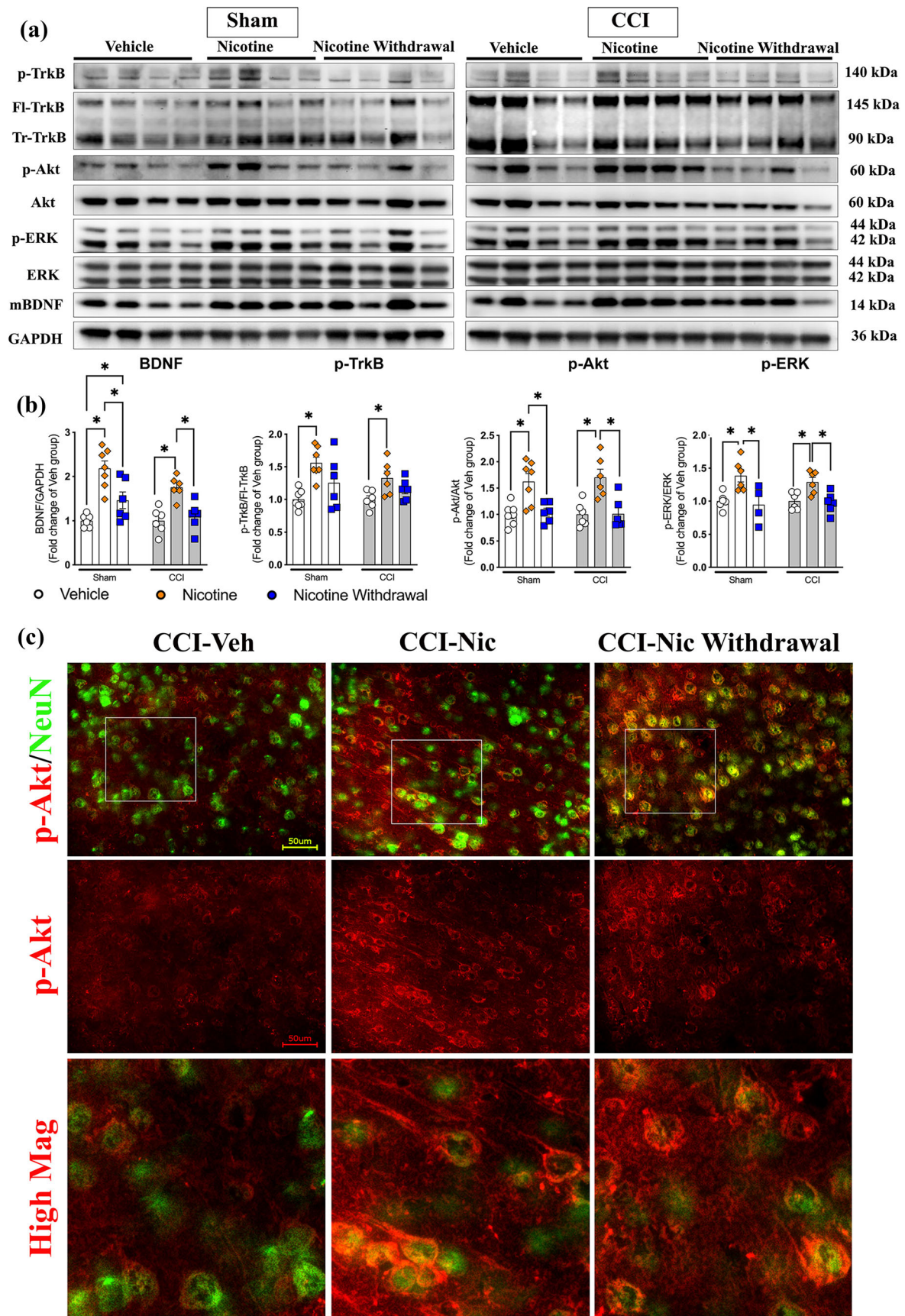


FIGURE 6 Legend on next page.

significant improvement in nestlet usage and nesting score compared to CCI-Veh group (Figure 3a,b). To further identify the time course of functional recovery, a separate cohort was used to track nesting performance biweekly. As shown in Figure 3c, an increasing trend in percent nestlet use ( $P = 0.09$ ) was observed as early as post-exposure Week 3, and a significant enhancement in nestlet usage was detected at post-exposure Week 5. Histological analyses of cortical tissue damage using Nissl stain revealed that while neuron number in the CCI-Veh group significantly decreased compared to Sham-Veh group, The CCI-Nic group showed a significantly higher neuron count compared to that of CCI-Veh group (Figure 3d-f). No significant difference was observed between CCI-Nic group and CCI-Nic withdrawal group. Together, our data suggest that nicotine exposure could significantly enhance long-term sensorimotor functional recovery after CCI.

### 3.4 | Withdrawal from chronic nicotine exposure adversely affects social approach behaviour in CCI mice

One of the most common symptoms observed in TBI patients is social maladjustment (Walz et al., 2009). However, baseline comparison of pre-exposure social preference showed no significant difference between Sham and CCI mice, and the social preference index for both groups fell within the normal range (Figure 4b) (Rein et al., 2020). The mice were then randomized to Veh, Nic and Nic withdrawal groups to ensure all groups exhibited similar interaction time with the stranger mouse and the object (Figure 4c). As shown in Figure 4d, after exposure, both Sham-Nic and CCI-Withdrawal groups showed no difference in time interacted with the stranger mouse and the object, suggesting that nicotine exposure suppressed social behaviour in Sham operated mice while nicotine withdrawal inhibited social behaviour in the CCI mice. We further compared pre- and post-exposure social preference indices (Figure 4e) and observed a significant decrease in social preference in the CCI-Nic Withdrawal group, suggesting a compounding effect of nicotine withdrawal and CCI on social approach behaviour.

### 3.5 | Chronic nicotine exposure increases mBDNF expression and activates associated downstream pro-survival signalling in the cortex

Since BDNF expression is regulated by various neurotransmitter systems that are sensitive to nicotine (Knipper et al., 1994; Li et al., 2014), we examined BDNF expression and its associated

signalling proteins in the cortex. As shown in Figure 5a,b, ipsilateral cortical tissue from Sham-Nic mice showed significantly increased mature BDNF (mBDNF) expression compared to both the Sham-Veh and Sham-Nic withdrawal groups, findings supported by a previous study that reported nicotine treatment increased mBDNF expression in the hippocampus (Lee et al., 2012). Corresponding to up-regulated mBDNF expression, we detected increased phosphorylated tyrosine receptor kinase B (p-TrkB), p-Akt and p-Erk expression in the Sham-Nic group, compared to that of the Sham-Veh and Sham-Nic withdrawal groups, confirming the activation of the BDNF-TrkB signalling pathway triggered by chronic nicotine exposure. Similar to what was observed within Sham groups, ipsilateral cortical tissue from CCI-Nic mice exhibited significantly elevated mBDNF, p-TrkB, p-AKT and p-Erk expression compared to the CCI-Veh and CCI-Nic withdrawal groups (Figures 5a,b), suggesting a nicotine-induced upregulation in BDNF signalling despite extensive damage to the ipsilateral cortex. No difference was observed in mBDNF, p-TrkB, p-Akt and p-Erk expression between Sham-Veh and CCI-Veh groups (Figure S2). Since Immunoblotting could not identify changes in specific subregions of the cortex nor cell types that contribute to the increased BDNF expression, we further performed immunostaining of BDNF and NeuN. As shown in Figure 5c (top three rows), while CCI-Veh and Sham-Veh presented a similar pattern of weak and sparse BDNF signals in a few cells, the CCI-Nic group showed a strong BDNF staining within multiple NeuN-positive neurons located in the perilesional area (Figure 5c bottom row).

A similar pattern of upregulation of mBDNF and associated downstream proteins was observed in the contralateral cortex of Sham-Nic and CCI-Nic mice (Figure 6a,b), revealing a global increase in BDNF-TrkB signalling due to chronic nicotine exposure. Furthermore, immunostaining revealed that p-Akt was colocalized with NeuN-positive neurons in the contralateral S1 cortex of CCI-Nic mice (Figure 6c), indicating activation of neuronal Akt signalling, a pro-growth and pro-survival signalling pathway that affords beneficial effects in multiple neurological disorders. Additional Immunoblotting of cortical tissue revealed that the up-regulated mBDNF and downstream signalling proteins maintained at a high level even at 1 week after nicotine cessation which gradually returned to baseline level at 2 weeks post cessation of nicotine (Figure S3).

### 3.6 | Chronic nicotine exposure attenuates microglia-mediated chronic neuroinflammation in CCI mice

TBI is known to increase the proliferation and activation of microglia (Acosta et al., 2013). Nicotine, on the other hand, has been

**FIGURE 6** Chronic nicotine exposure increases mBDNF expression and up-regulates BDNFTrkB signalling in the contralateral cortex. (a) Immunoblot analyses of the expression of p-TrkB, TrkB, p-Akt, Akt, p-ERK, ERK, mBDNF and GAPDH in contralateral cortex of Sham and controlled cortical impact (CCI) mice. (b) Quantification of above blots in (a),  $n = 6-7$  per group. (c) Representative immunofluorescence images of p-Akt (red) and neuronal marker neuronal nuclear protein (NeuN) (green). Scale bar, 500  $\mu\text{m}$ . Data are analysed using one-way ANOVA followed post hoc Fisher's LSD tests. Data are presented as mean  $\pm$  SEM. Significance was assumed when  $*P < 0.05$ . Veh, Vehicle; Nic, nicotine.

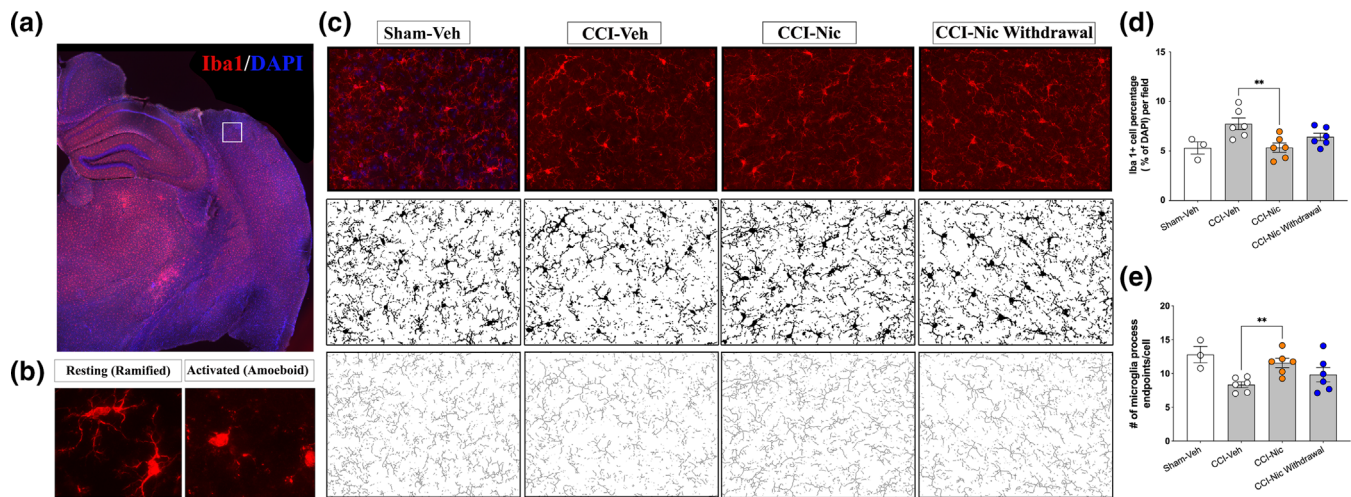


**FIGURE 7** Chronic nicotine exposure mitigates microglia-mediated neuroinflammation in controlled cortical impact (CCI) mice. (a) Representative image of Iba1 (red) staining in the ipsilateral brain. DAPI (blue) indicates the nucleus. The boxed area indicates the perilesion region where microglia count and morphology were examined. (b) Representative images of resting (ramified) vs. activated (deramified) microglial morphology. (c) High-magnification full micrographs of Iba1 staining in the perilesion primary sensory cortex. Corresponding binary and skeletonized images are shown in the middle and bottom rows. (d) Percentage of Iba1+ cells in the counting field (n = 3 for Sham-Vehicle group, n = 6 for all CCI groups). (e) Number of microglia process endpoints per cell. Data are analysed using one-way ANOVA followed by post hoc Fisher's LSD tests. Data are presented as mean ± SEM. Significance was assumed when \*P < 0.05. No statistical comparison was made with the sham group, since n < 5. Veh, Vehicle; Nic, nicotine.

shown to regulate microglia activation and suppress inflammation in the CNS via interactions with  $\alpha 7$  acetylcholine receptors (Noda & Kobayashi, 2017; Shytle et al., 2004; Zhang et al., 2017). Thus, we performed Iba-1 immunolabelling to determine the effects of chronic nicotine exposure on CCI-induced chronic neuroinflammation. As shown in Figure 7b, while microglia in the Sham-Veh group maintained a ramified morphology, reactive microglia with a distinct amoeboid shape were found in all three CCI groups, confirming persistent microglia-mediated neuroinflammation at 2 months post CCI. Quantification of the Iba1-positive cells in the perilesion primary sensory cortex (Figure 7c,d) showed that the CCI-Veh group presented an increased microglia count compared to that of the exploratory Sham-Veh group. Most importantly, the perilesion cortex of nicotine-exposed mice showed a significantly decreased microglia count compared to the CCI-Veh group. A similar decreasing trend ( $P = 0.067$ ) in the microglial count was observed in the CCI-Nic Withdrawal group, suggesting that chronic nicotine exposure via E-cig alleviated microglia-mediated neuroinflammation following CCI. Further analysis of microglia morphology by quantifying the number of process endpoints per cell showed decreased process endpoints in the perilesional cortex of CCI-Veh group when compared to the exploratory Sham-Veh group (Figure 7c,e). Importantly, process endpoint analysis revealed a significantly more ramified microglia morphology in the CCI-Nic group compared to that of the CCI-Veh group. No difference in microglial ramification was detected between the CCI-Veh and CCI-Nic withdrawal groups, suggesting that continuous administration of nicotine is necessary to drive and maintain a more ramified microglia morphology following experimental TBI.

## 4 | DISCUSSION

The current study utilized a clinically relevant full-body E-cig vapour exposure system to investigate the effects of chronic nicotine exposure on traumatic brain injury. While several  $\alpha 7$ -nAChRs agonists have been developed as pro-cognitive agents for neurological disorders like schizophrenia (Lieberman et al., 2013) and Alzheimer's Disease (Gault et al., 2015; Roberts et al., 2021), this study is the first to demonstrate the neuroprotective effect of nicotine in preserving sensorimotor function after TBI. Our results revealed that chronic nicotine exposure via E-cig inhalation significantly improved long-term sensorimotor functional recovery in CCI mice. This improvement was accompanied by an increase in cortical expression of mBDNF and upregulation of BDNF/TrkB-associated pro-survival signalling pathways, including p-Erk and p-Akt. Notably, the increased BDNF and p-Akt signalling were predominantly observed in neurons. Additionally, chronic nicotine exposure alleviated microglia-mediated chronic neuroinflammation following CCI. However, it is noteworthy that nicotine withdrawal significantly impeded social approach behaviour in the CCI mice, indicating a need for further exploration of withdrawal effects in the context of TBI recovery.

Individuals with severe TBI suffer from long-lasting sensorimotor deficits due to significant neuronal loss, diffuse axonal injuries and chronic neuroinflammation. While studies using moderate and diffuse TBI rodent models showed that nesting behaviour could recover to baseline level at 7 days post CCI (Muccigrosso et al., 2016), severe TBI models presented persistent nesting deficits that last for months (Ritzel et al., 2020). In this current study, both the CCI-Nic and the CCI-Nic Withdrawal groups showed significantly enhanced function

recovery, suggesting that the functional improvement is not dependent on nicotine's transient modulating effects on **dopamine** (DA)-mediated motivation change but a true improvement in long-term functional recovery after CCI. No significant difference was observed in the lesion size among the three CCI groups (Figure S4), a result expected as nicotine exposure did not begin until 7 days post-injury. Together, these results suggest that the observed beneficial effect of nicotine on nesting performance is possibly achieved by alleviating secondary injuries such as neurodegeneration and/or chronic neuroinflammation during the chronic phase of TBI. Considering that an upward trend in nesting performance could be detected as early as 3 weeks post-exposure, future studies that examine whether a shorter nicotine treatment could achieve similar functional recovery while avoiding nicotine dependence and associated symptoms may provide valuable information for the development of nicotine-based therapy for TBI patients. Additionally, given that several animal studies suggested that nicotine treatment before and immediately post-injury could provide potential benefits for TBI-induced deficits by compensating impaired cholinergic, serotonergic, and dopaminergic signalling (Lee et al., 2012; Shin et al., 2012; Verbois, Hopkins, et al., 2003; Verbois, Scheff, & Pauly, 2003), it would be interesting to investigate the effect of activation of nicotinic receptors at an earlier time point after TBI on BDNF related signalling pathway and sensorimotor function recovery.

The open field test has long been used to measure anxiety-related behaviour in rodents (Bailey & Crawley, 2009) since mice generally display strong centre-avoidance behaviour (thigmotaxis). Our study demonstrated that nicotine induces hyperlocomotion along with decreased thigmotaxis in mice from the CCI-Nic group compared to the CCI-Veh and CCI-Nic withdrawal groups. Increased exploration of the anxiogenic centre may suggest an attenuated response to environmental stressors in TBI-Nic mice. We suspect such behavioural change could be due to an impaired serotonin system following nicotine exposure (Ribeiro et al., 1993), a system that plays a key role in modulating anxiety (Gordon & Hen, 2004). This is consistent with previous research that established the anxiolytic effect of nicotine. Importantly, no changes in locomotion and thigmotactic behaviour were observed in the CCI-Nic withdrawal group, indicating that the effects of nicotine on psychomotor behaviour are likely short-lived. Together, these results could possibly explain the prevalent use of nicotine-containing products among TBI patients as a form of self-medication to cope with negative affective states caused by brain injuries (Brown, 2010; Silva et al., 2018).

BDNF, an important neurotrophin that binds to TrkB receptors, is well-established for its role in enhancing neuronal survival in the injured CNS (Gustafsson et al., 2021; Wurzelmann et al., 2017). Nicotine, by binding to nicotinic receptors, has been shown to interact with the BDNF-TrkB pathway (Serres & Carney, 2006). However, while some studies claimed that chronic nicotine treatment could increase BDNF mRNA or protein expression in the adult rodent brain (Alasmari et al., 2021; Kenny et al., 2000; Naha et al., 2018), others reported no change or decreased BDNF mRNA/protein expression after chronic nicotine treatment (Aleisa et al., 2006; Ortega

et al., 2013). In the setting of TBI, Lee and colleagues have demonstrated that chronic exposure to cigarette smoke before TBI induces upregulation of hippocampal BDNF mRNA and affords neuroprotective effects (Lee et al., 2012). The current study further demonstrates that chronic nicotine exposure, begun one week after the initial injury, still increased cortical mBDNF expression in the perilesion cortex. Importantly, the increased Erk and Akt activation suggests that, even in the setting of TBI, which has been shown to induce significant deficits in Erk activation (Atkins et al., 2009), chronic nicotine exposure still induced activation of Erk and Akt, two crucial kinases responsible for promoting neuronal survival. Furthermore, immunostaining confirmed that the up-regulated p-Akt signals in the perilesion area are mostly localized within the neuronal population, which could explain the preservation of perilesion neurons and greater functional recovery observed in nicotine-exposed CCI mice.

Microglia activation is an important pathological hallmark of TBI. Mounting evidence has shown that microglia activation can persist beyond months to years in the rodent TBI model, contributing to accelerated neurodegeneration and encephalopathy (Simon et al., 2017). The cholinergic anti-inflammatory pathway, which depends on the activation of  $\alpha 7$  nACh receptors on immune cells, plays an important role in regulating CNS inflammation (Shytle et al., 2004). Furthermore, activation of microglial  $\alpha 7$  nACh receptors has been shown to promote the conversion of pro-inflammatory microglia to the anti-inflammatory type (Zhang et al., 2017). Consistent with these previous findings, the current study revealed significantly increased microglia process endpoints in the CCI-Nic group compared to that of CCI-Veh and CCI-Nic withdrawal groups, suggesting a less reactive phenotype of microglia in nicotine-treated mice. Together, our data suggest that post-injury nicotine exposure attenuates neuroinflammation by suppressing microgliosis in the perilesional cortex of CCI mice, which may, in part, facilitate recovery of sensorimotor function.

Although nicotine treatment affords beneficial effects on sensorimotor recovery after TBI, the current study also demonstrated significant inhibition of SA behaviour in CCI-Nic withdrawal mice. Such inhibition may reflect anhedonia and/or a disrupted mental state, symptoms that are closely associated with nicotine withdrawal (Mayer et al., 2001). The unaltered social behaviour observed in the CCI-Veh group can be attributed to the CCI model used in the current setting, which does not directly damage the medial prefrontal cortex and amygdala, two brain regions that are primarily responsible for modulating social behaviour (Adolphs, 2009). The absence of nicotine's inhibitory effect in the CCI-Nic group may indicate that, in the injured CNS, nicotine-mediated activation of native cholinergic signalling is disrupted due to extensive damage in the cortex and hippocampus (Schmidt & Grady, 1995; Shin & Dixon, 2015). Together, these findings suggest that, while chronic nicotine exposure provides neuroprotective effect for TBI, nicotine withdrawal could adversely affect social behaviour in TBI patients. Furthermore, preclinical and clinical studies have suggested that increased brain BDNF levels may be related to drug dependence (Vargas-Perez et al., 2014). Therefore, the potential side effects associated with chronic nicotine exposure must

be considered while exploring the pharmacological utility of nicotinic receptor agonism to treat brain injury and other neurodegenerative conditions.

One limitation of this study is that we exclusively investigated the biochemistry change in perilesion cortical tissue, but the E-cig nicotine exposure model likely affects the whole CNS, especially regions that rely on DA signalling such as the basal ganglia circuitry (Shin et al., 2012). Further investigations on the effects of chronic nicotine exposure on the dopaminergic pathway in the injured brain may provide additional insights into the therapeutic potential of nicotine.

In conclusion, the present study showed that post-injury chronic nicotine exposure via E-cigs facilitated long-term functional recovery from CCI-induced sensorimotor deficits by upregulating neuroprotective BDNF–TrkB signalling and alleviating microglia-mediated neuroinflammation. However, nicotine withdrawal induced abnormal social behaviours in CCI mice. Further investigation into specific treatment regimens (delivery route, dose, and duration) of nicotine and selective  $\alpha 7$  nACh receptors agonists in the setting of TBI could provide valuable information on potential therapeutic targets for traumatic brain injury and other forms of neurodegeneration.

#### AUTHOR CONTRIBUTIONS

Conceptualization: B. P. Head and S. Wang. Methodology for E-cig exposure and SA: E. Breen and S. Powell. Behaviour test: N. Kleschevnikova and T. Duong. Immunoblot and Immunofluorescence: D. Wang, H. Wang, X. Li and W. Li. Formal analysis: S. Wang, D. Wang and S. Powell. Original writing: D. Wang and S. Wang. Review and editing: S. Wang, S. Powell, B. Head and H. Patel. All authors have read and approved the final version of the manuscript.

#### CONFLICT OF INTEREST STATEMENT

The authors declare no conflicts of interest.

#### DATA AVAILABILITY STATEMENT

The data that support the findings of this study are available from the corresponding author upon reasonable request.

#### DECLARATION OF TRANSPARENCY AND SCIENTIFIC RIGOUR

This Declaration acknowledges that this paper adheres to the principles for transparent reporting and scientific rigour of preclinical research as stated in the *BJP* guidelines for [Natural Products Research](#), [Design and Analysis](#), [Immunoblotting and Immunochemistry](#) and [Animal Experimentation](#), and as recommended by funding agencies, publishers and other organizations engaged with supporting research.

#### DECLARATIONS

H. H. P. and B. P. H. hold equity and are non-paid consultants with Eikonoklastes Therapeutics LLC.

#### REFERENCES

Acosta, S. A., Tajiri, N., Shinozuka, K., Ishikawa, H., Grimmig, B., Diamond, D. M., Sanberg, P. R., Bickford, P. C., Kaneko, Y., &

- Borlongan, C. V. (2013). Long-term upregulation of inflammation and suppression of cell proliferation in the brain of adult rats exposed to traumatic brain injury using the controlled cortical impact model. *PLoS ONE*, 8(1), e53376. <https://doi.org/10.1371/journal.pone.0053376>
- Adolphs, R. (2009). The social brain: Neural basis of social knowledge. *Annual Review of Psychology*, 60, 693–716. <https://doi.org/10.1146/annurev.psych.60.110707.163514>
- Alasmari, F., Alotibi, F. M., Alqahtani, F., Alshammari, T. K., Kadi, A. A., Alghamdi, A. M., Allahem, B. S., Alasmari, A. F., Alsharari, S. D., Al-Rejaie, S. S., & Alshammari, M. A. (2022). Effects of chronic inhalation of electronic cigarette vapor containing nicotine on Neurobehaviors and pre/postsynaptic neuron markers. *Toxics*, 10(6), 338. <https://doi.org/10.3390/toxics10060338>
- Alasmari, F., Crotty Alexander, L. E., Hammad, A. M., Horton, A., Alhaddad, H., Schiefer, I. T., Shin, J., Moshensky, A., & Sari, Y. (2021). E-cigarette aerosols containing nicotine modulate nicotinic acetylcholine receptors and astroglial glutamate transporters in mesocorticolimbic brain regions of chronically exposed mice. *Chemico-Biological Interactions*, 333, 109308. <https://doi.org/10.1016/j.cbi.2020.109308>
- Aleisa, A. M., Alzoubi, K. H., & Alkadhi, K. A. (2006). Nicotine prevents stress-induced enhancement of long-term depression in hippocampal area CA1: Electrophysiological and molecular studies. *Journal of Neuroscience Research*, 83(2), 309–317. <https://doi.org/10.1002/jnr.20716>
- Alexander, S. P. H., Fabbro, D., Kelly, E., et al. (2023a). The Concise Guide to PHARMACOLOGY 2023/24: Catalytic receptors. *Br J Pharmacol*, 180, S241–S288. <https://doi.org/10.1111/bph.16180>
- Alexander, S. P. H., Fabbro, D., Kelly, E., et al. (2023b). The Concise Guide to PHARMACOLOGY 2023/24: Enzymes. *Br J Pharmacol*, 180, S289–S373. <https://doi.org/10.1111/bph.16181>
- Alexander, S. P. H., Mathie, A. A., Peters, J. A., et al. (2023). (2023). The Concise Guide to PHARMACOLOGY 2023/24: Ion channels. *Br J Pharmacol*, 180, S145–S222. <https://doi.org/10.1111/bph.16181>
- Alexander, S. P. H., Roberts, R. E., Broughton, B. R. S., Sobey, C. G., George, C. H., Stanford, S. C., ... Ahluwalia, A. (2018). Goals and practicalities of immunoblotting and immunohistochemistry: A guide for submission to the British Journal of Pharmacology. *British Journal of Pharmacology*, 175, 407–411. <https://doi.org/10.1111/bph.14112>
- Atkins, C. M., Faló, M. C., Alonso, O. F., Bramlett, H. M., & Dietrich, W. D. (2009). Deficits in ERK and CREB activation in the hippocampus after traumatic brain injury. *Neuroscience Letters*, 459(2), 52–56. <https://doi.org/10.1016/j.neulet.2009.04.064>
- Bailey, K., & Crawley, J. (2009). In J. J. Buccafusco (Ed.), *Methods of behavior analysis in neuroscience* (2nd ed.). CRC Press/Taylor & Francis.
- Brett, B. L., Gardner, R. C., Godbout, J., Dams-O'Connor, K., & Keene, C. D. (2022). Traumatic brain injury and risk of neurodegenerative disorder. *Biological Psychiatry*, 91(5), 498–507. <https://doi.org/10.1016/j.biopsych.2021.05.025>
- Brown, D. W. (2010). Smoking prevalence among US veterans. *Journal of General Internal Medicine*, 25(2), 147–149. <https://doi.org/10.1007/s11606-009-1160-0>
- Castillo-Rolon, D., Ramirez-Sanchez, E., Arenas-Lopez, G., Garduno, J., Hernandez-Gonzalez, O., Mihailescu, S., & Hernandez-Lopez, S. (2020). Nicotine increases spontaneous glutamate release in the Rostromedial tegmental nucleus. *Frontiers in Neuroscience*, 14, 604583. <https://doi.org/10.3389/fnins.2020.604583>
- Curtis, M. J., Alexander, S. P. H., Cirino, G., George, C. H., Kendall, D. A., Insel, P. A., Izzo, A. A., Ji, Y., Panettieri, R. A., Patel, H. H., Sobey, C. G., Stanford, S. C., Stanley, P., Stefanska, B., Stephens, G. J., Teixeira, M. M., Vergnolle, N., & Ahluwalia, A. (2022). Planning experiments: Updated guidance on experimental design and analysis and their reporting III. *British Journal of Pharmacology*, 179(15), 3907–3913. <https://doi.org/10.1111/bph.15868>
- Deacon, R. M. (2006). Assessing nest building in mice. *Nature Protocols*, 1(3), 1117–1119. <https://doi.org/10.1038/nprot.2006.170>

- Dineley, K. T., Pandya, A. A., & Yakel, J. L. (2015). Nicotinic ACh receptors as therapeutic targets in CNS disorders. *Trends in Pharmacological Sciences*, 36(2), 96–108. <https://doi.org/10.1016/j.tips.2014.12.002>
- Durazzo, T. C., Abadjian, L., Kincaid, A., Bilovsky-Muniz, T., Boreta, L., & Gauger, G. E. (2013). The influence of chronic cigarette smoking on neurocognitive recovery after mild traumatic brain injury. *Journal of Neurotrauma*, 30(11), 1013–1022. <https://doi.org/10.1089/neu.2012.2676>
- Egawa, J., Schilling, J. M., Cui, W., Posadas, E., Sawada, A., Alas, B., Zemljic-Harper, A. E., Fannon-Pavlich, M. J., Mandyam, C. D., Roth, D. M., Patel, H. H., Patel, P. M., & Head, B. P. (2017). Neuron-specific caveolin-1 overexpression improves motor function and preserves memory in mice subjected to brain trauma. *The FASEB Journal*, 31(8), 3403–3411. <https://doi.org/10.1096/fj.201601288RRR>
- Fleming, S. M., Salcedo, J., Fernagut, P. O., Rockenstein, E., Masliah, E., Levine, M. S., & Chesselet, M. F. (2004). Early and progressive sensorimotor anomalies in mice overexpressing wild-type human alpha-synuclein. *The Journal of Neuroscience*, 24(42), 9434–9440. <https://doi.org/10.1523/JNEUROSCI.3080-04.2004>
- Flouris, A. D., Chorti, M. S., Poulanioti, K. P., Jamurtas, A. Z., Kostikas, K., Tzatzarakis, M. N., Wallace Hayes, A., Tsatsakis, A. M., & Koutedakis, Y. (2013). Acute impact of active and passive electronic cigarette smoking on serum cotinine and lung function. *Inhalation Toxicology*, 25(2), 91–101. <https://doi.org/10.3109/08958378.2012.758197>
- Gaskill, B. N., Gordon, C. J., Pajor, E. A., Lucas, J. R., Davis, J. K., & Garner, J. P. (2012). Heat or insulation: Behavioral titration of mouse preference for warmth or access to a nest. *PLoS ONE*, 7(3), e32799. <https://doi.org/10.1371/journal.pone.0032799>
- Gault, L. M., Ritchie, C. W., Robieson, W. Z., Pritchett, Y., Othman, A. A., & Lenz, R. A. (2015). A phase 2 randomized, controlled trial of the alpha7 agonist ABT-126 in mild-to-moderate Alzheimer's dementia. *Alzheimer's Dement (N Y)*, 1(1), 81–90. <https://doi.org/10.1016/j.trci.2015.06.001>
- Gordon, J. A., & Hen, R. (2004). The serotonergic system and anxiety. *Neuromolecular Medicine*, 5(1), 27–40. <https://doi.org/10.1385/NMM:5:1:027>
- Gustafsson, D., Klang, A., Thams, S., & Rostami, E. (2021). The role of BDNF in experimental and clinical traumatic brain injury. *International Journal of Molecular Sciences*, 22(7), 3582. <https://doi.org/10.3390/ijms22073582>
- Jobson, C. L. M., Renard, J., Szkudlarek, H., Rosen, L. G., Pereira, B., Wright, D. J., Rushlow, W., & Laviolette, S. R. (2019). Adolescent nicotine exposure induces dysregulation of Mesocorticolimbic activity states and depressive and anxiety-like prefrontal cortical molecular phenotypes persisting into adulthood. *Cerebral Cortex*, 29(7), 3140–3153. <https://doi.org/10.1093/cercor/bhy179>
- Jones, K., & Salzman, G. A. (2020). The vaping epidemic in adolescents. *Missouri Medicine*, 117(1), 56–58.
- Kenny, P. J., File, S. E., & Rattray, M. (2000). Acute nicotine decreases, and chronic nicotine increases the expression of brain-derived neurotrophic factor mRNA in rat hippocampus. *Brain Research. Molecular Brain Research*, 85(1–2), 234–238. [https://doi.org/10.1016/s0169-328x\(00\)00246-1](https://doi.org/10.1016/s0169-328x(00)00246-1)
- Knipper, M., da Penha Berzaghi, M., Blochl, A., Breer, H., Thoenen, H., & Lindholm, D. (1994). Positive feedback between acetylcholine and the neurotrophins nerve growth factor and brain-derived neurotrophic factor in the rat hippocampus. *The European Journal of Neuroscience*, 6(4), 668–671. <https://doi.org/10.1111/j.1460-9568.1994.tb00312.x>
- Lechasseur, A., Altmejd, S., Turgeon, N., Buonanno, G., Morawska, L., Brunet, D., Duchaine, C., & Morissette, M. C. (2019). Variations in coil temperature/power and e-liquid constituents change size and lung deposition of particles emitted by an electronic cigarette. *Physiological Reports*, 7(10), e14093. <https://doi.org/10.14814/phy2.14093>
- Lee, I. N., Lin, M. H., Chung, C. Y., Lee, M. H., Weng, H. H., & Yang, J. T. (2012). Chronic cigarette smoke exposure enhances brain-derived neurotrophic factor expression in rats with traumatic brain injury. *Metabolic Brain Disease*, 27(2), 197–204. <https://doi.org/10.1007/s11011-012-9294-x>
- Li, X., Semenova, S., D'Souza, M. S., Stoker, A. K., & Markou, A. (2014). Involvement of glutamatergic and GABAergic systems in nicotine dependence: Implications for novel pharmacotherapies for smoking cessation. *Neuropharmacology*, 76(Pt B(0 0)), 554–565. <https://doi.org/10.1016/j.neuropharm.2013.05.042>
- Lieberman, J. A., Dunbar, G., Segreti, A. C., Girgis, R. R., Seoane, F., Beaver, J. S., Duan, N., & Hosford, D. A. (2013). A randomized exploratory trial of an alpha-7 nicotinic receptor agonist (TC-5619) for cognitive enhancement in schizophrenia. *Neuropsychopharmacology*, 38(6), 968–975. <https://doi.org/10.1038/npp.2012.259>
- Lilley, E., Stanford, S. C., Kendall, D. E., Alexander, S. P. H., Cirino, G., Docherty, J. R., George, C. H., Insel, P. A., Izzo, A. A., Ji, Y., Panettieri, R. A., Sobey, C. G., Stefanska, B., Stephens, G., Teixeira, M., & Ahluwalia, A. (2020). ARRIVE 2.0 and the British Journal of Pharmacology: Updated guidance for 2020. *British Journal of Pharmacology*, 177(16), 3611–3616. <https://doi.org/10.1111/bph.15178>
- Mayer, S. A., Chong, J. Y., Ridgway, E., Min, K. C., Commichau, C., & Bernardini, G. L. (2001). Delirium from nicotine withdrawal in neuro-ICU patients. *Neurology*, 57(3), 551–553. <https://doi.org/10.1212/wnl.57.3.551>
- Muccigrosso, M. M., Ford, J., Benner, B., Moussa, D., Burnsides, C., Fenn, A. M., Popovich, P. G., Lifshitz, J., Walker, F. R., Eiferman, D. S., & Godbout, J. P. (2016). Cognitive deficits develop 1month after diffuse brain injury and are exaggerated by microglia-associated reactivity to peripheral immune challenge. *Brain, Behavior, and Immunity*, 54, 95–109. <https://doi.org/10.1016/j.bbi.2016.01.009>
- Naha, N., Gandhi, D. N., Gautam, A. K., & Prakash, J. R. (2018). Nicotine and cigarette smoke modulate Nrf2-BDNF-dopaminergic signal and neurobehavioral disorders in adult rat cerebral cortex. *Human & Experimental Toxicology*, 37(5), 540–556. <https://doi.org/10.1177/0960327117698543>
- Noda, M., & Kobayashi, A. I. (2017). Nicotine inhibits activation of microglial proton currents via interactions with alpha7 acetylcholine receptors. *The Journal of Physiological Sciences*, 67(1), 235–245. <https://doi.org/10.1007/s12576-016-0460-5>
- Ortega, L. A., Tracy, B. A., Gould, T. J., & Parikh, V. (2013). Effects of chronic low- and high-dose nicotine on cognitive flexibility in C57BL/6J mice. *Behavioural Brain Research*, 238, 134–145. <https://doi.org/10.1016/j.bbr.2012.10.032>
- Paumier, K. L., Sukoff Rizzo, S. J., Berger, Z., Chen, Y., Gonzales, C., Kaftan, E., Li, L., Lotarski, S., Monaghan, M., Shen, W., Stolyar, P., Vasilyev, D., Zaleska, M., Hirst, D. W., & Dunlop, J. (2013). Behavioral characterization of A53T mice reveals early and late stage deficits related to Parkinson's disease. *PLoS ONE*, 8(8), e70274. <https://doi.org/10.1371/journal.pone.0070274>
- Percie du Sert, N., Hurst, V., Ahluwalia, A., Alam, S., Avey, M. T., Baker, M., Browne, W. J., Clark, A., Cuthill, I. C., Dirnagl, U., Emerson, M., Garner, P., Holgate, S. T., Howells, D. W., Karp, N. A., Lazic, S. E., Lidster, K., MacCallum, C. J., Macleod, M., ... Würbel, H. (2020). The ARRIVE guidelines 2.0: Updated guidelines for reporting animal research. *British Journal of Pharmacology*, 177(16), 3617–3624. <https://doi.org/10.1111/bph.15193>
- Rao, R. K., McConnell, D. D., & Litofsky, N. S. (2022). The impact of cigarette smoking and nicotine on traumatic brain injury: A review. *Brain Injury*, 36(1), 1–20. <https://doi.org/10.1080/02699052.2022.2034186>
- Rein, B., Ma, K., & Yan, Z. (2020). A standardized social preference protocol for measuring social deficits in mouse models of autism. *Nature Protocols*, 15(10), 3464–3477. <https://doi.org/10.1038/s41596-020-0382-9>



- Ribeiro, E. B., Bettiker, R. L., Bogdanov, M., & Wurtman, R. J. (1993). Effects of systemic nicotine on serotonin release in rat brain. *Brain Research*, 621(2), 311–318. [https://doi.org/10.1016/0006-8993\(93\)90121-3](https://doi.org/10.1016/0006-8993(93)90121-3)
- Ritzel, R. M., Li, Y., He, J., Khan, N., Doran, S. J., Faden, A. I., & Wu, J. (2020). Sustained neuronal and microglial alterations are associated with diverse neurobehavioral dysfunction long after experimental brain injury. *Neurobiology of Disease*, 136, 104713. <https://doi.org/10.1016/j.nbd.2019.104713>
- Roberts, J. P., Stokoe, S. A., Sathler, M. F., Nichols, R. A., & Kim, S. (2021). Selective coactivation of alpha7- and alpha4beta2-nicotinic acetylcholine receptors reverses beta-amyloid-induced synaptic dysfunction. *The Journal of Biological Chemistry*, 296, 100402. <https://doi.org/10.1016/j.jbc.2021.100402>
- Schmidt, R. H., & Grady, M. S. (1995). Loss of forebrain cholinergic neurons following fluid-percussion injury: Implications for cognitive impairment in closed head injury. *Journal of Neurosurgery*, 83(3), 496–502. <https://doi.org/10.3171/jns.1995.83.3.0496>
- Serres, F., & Carney, S. L. (2006). Nicotine regulates SH-SY5Y neuroblastoma cell proliferation through the release of brain-derived neurotrophic factor. *Brain Research*, 1101(1), 36–42. <https://doi.org/10.1016/j.brainres.2006.05.023>
- Shin, S. S., Bray, E. R., & Dixon, C. E. (2012). Effects of nicotine administration on striatal dopamine signaling after traumatic brain injury in rats. *Journal of Neurotrauma*, 29(5), 843–850. <https://doi.org/10.1089/neu.2011.1966>
- Shin, S. S., & Dixon, C. E. (2015). Alterations in cholinergic pathways and therapeutic strategies targeting cholinergic system after traumatic brain injury. *Journal of Neurotrauma*, 32(19), 1429–1440. <https://doi.org/10.1089/neu.2014.3445>
- Shytle, R. D., Mori, T., Townsend, K., Vendrame, M., Sun, N., Zeng, J., Ehrhart, J., Silver, A. A., Sanberg, P. R., & Tan, J. (2004). Cholinergic modulation of microglial activation by alpha 7 nicotinic receptors. *Journal of Neurochemistry*, 89(2), 337–343. <https://doi.org/10.1046/j.1471-4159.2004.02347.x>
- Silva, M. A., Belanger, H. G., Dams-O'Connor, K., Tang, X., McKenzie-Hartman, T., & Nakase-Richardson, R. (2018). Prevalence and predictors of tobacco smoking in veterans and service members following traumatic brain injury rehabilitation: A VA TBIMS study. *Brain Injury*, 32(8), 994–999. <https://doi.org/10.1080/02699052.2018.1468576>
- Simon, D. W., McGeachy, M. J., Bayir, H., Clark, R. S., Loane, D. J., & Kochanek, P. M. (2017). The far-reaching scope of neuroinflammation after traumatic brain injury. *Nature Reviews. Neurology*, 13(3), 171–191. <https://doi.org/10.1038/nrneurol.2017.13>
- Vargas-Perez, H., Bahi, A., Bufalino, M. R., Ting, A. K. R., Maal-Bared, G., Lam, J., Fahmy, A., Clarke, L., Blanchard, J. K., Larsen, B. R., Steffensen, S., Dreyer, J. L., & van der Kooy, D. (2014). BDNF signaling in the VTA links the drug-dependent state to drug withdrawal aversions. *The Journal of Neuroscience*, 34(23), 7899–7909. <https://doi.org/10.1523/JNEUROSCI.3776-13.2014>
- Verbois, S. L., Hopkins, D. M., Scheff, S. W., & Pauly, J. R. (2003). Chronic intermittent nicotine administration attenuates traumatic brain injury-induced cognitive dysfunction. *Neuroscience*, 119(4), 1199–1208. [https://doi.org/10.1016/s0306-4522\(03\)00206-9](https://doi.org/10.1016/s0306-4522(03)00206-9)
- Verbois, S. L., Scheff, S. W., & Pauly, J. R. (2003). Chronic nicotine treatment attenuates alpha 7 nicotinic receptor deficits following traumatic brain injury. *Neuropharmacology*, 44(2), 224–233. [https://doi.org/10.1016/s0028-3908\(02\)00366-0](https://doi.org/10.1016/s0028-3908(02)00366-0)
- Walz, N. C., Yeates, K. O., Wade, S. L., & Mark, E. (2009). Social information processing skills in adolescents with traumatic brain injury: Relationship with social competence and behavior problems. *Journal of Pediatric Rehabilitation Medicine*, 2(4), 285–295. <https://doi.org/10.3233/PRM-2009-0094>
- Wang, S., Leem, J. S., Podvin, S., Hook, V., Kleschevnikov, N., Savchenko, P., Dhanani, M., Zhou, K., Kelly, I. C., Zhang, T., Miyano-hara, A., Nguyen, P., Kleschevnikov, A., Wagner, S. L., Trojanowski, J. Q., Roth, D. M., Patel, H. H., Patel, P. M., & Head, B. P. (2021). Synapsin-caveolin-1 gene therapy preserves neuronal and synaptic morphology and prevents neurodegeneration in a mouse model of AD. *Molecular Therapy - Methods & Clinical Development*, 21, 434–450. <https://doi.org/10.1016/j.omtm.2021.03.021>
- Wurzelmann, M., Romeika, J., & Sun, D. (2017). Therapeutic potential of brain-derived neurotrophic factor (BDNF) and a small molecular mimics of BDNF for traumatic brain injury. *Neural Regeneration Research*, 12(1), 7–12. <https://doi.org/10.4103/1673-5374.198964>
- Young, K., & Morrison, H. (2018). Quantifying microglia morphology from photomicrographs of immunohistochemistry prepared tissue using ImageJ. *Journal of Visualized Experiments*, (136), 57648. <https://doi.org/10.3791/57648>
- Yuan, D., Liu, C., Wu, J., & Hu, B. (2018). Nest-building activity as a reproducible and long-term stroke deficit test in a mouse model of stroke. *Brain and Behavior: a Cognitive Neuroscience Perspective*, 8(6), e00993. <https://doi.org/10.1002/brb3.993>
- Zhang, Q., Lu, Y., Bian, H., Guo, L., & Zhu, H. (2017). Activation of the alpha7 nicotinic receptor promotes lipopolysaccharide-induced conversion of M1 microglia to M2. *American Journal of Translational Research*, 9(3), 971–985.

## SUPPORTING INFORMATION

Additional supporting information can be found online in the Supporting Information section at the end of this article.

**How to cite this article:** Wang, D., Li, X., Li, W., Duong, T., Wang, H., Kleschevnikova, N., Patel, H. H., Breen, E., Powell, S., Wang, S., & Head, B. P. (2024). Nicotine inhalant via E-cigarette facilitates sensorimotor function recovery by upregulating neuronal BDNF-TrkB signalling in traumatic brain injury. *British Journal of Pharmacology*, 1–16. <https://doi.org/10.1111/bph.16395>